Monitoring paddy rice phenology using time series MODIS data over Jiangxi Province, China

Li Shihua[1*], Xiao Jiangtao[1], Ni Ping[1], Zhang Jing[2], Wang Hongshu[1], Wang Jingxian[1]

(1. *School of Resources and Environment, University of Electronic Science and Technology of China, Chengdu, 611731, China*; 2. *The National Remote Sensing Center of China, Beijing, 100036, China*)

Abstract: Paddy rice is one of the most important crops in the world. Accurate estimation and monitoring of paddy rice phenology is necessary for management and yield prediction. Remotely sensed time-series data are essential for estimation of crop phenology stages across large areas. Here, the paddy rice phenological stages (i.e., transplanting, tillering, heading, and harvesting) were detected in Jiangxi Province, China. A comparison study was conducted using ground observation data from 10 agricultural meteorological stations, collected between 2006 and 2008. The phenological stages were detected using Moderate Resolution Imaging Spectroradiometer (MODIS) time-series enhanced vegetation index (EVI) data. Savitzky–Golay filter and wavelet transform were used to reduce the noise in the time-series EVI data and reconstruct the smoothed EVI time-series profile. Key phenological stages of double-cropping rice were detected using the characteristics of the smoothed EVI profile. The root mean square errors (RMSEs) for each stage were ±10 days around the ground observation data. The results suggest that Savitzky–Golay filter and wavelet transform are promising approaches for reconstructing high-quality EVI time-series data. Moreover, the phenological stages of double-cropping rice could be detected using time-series MODIS EVI data smoothed by Savitzky–Golay filter and wavelet transform.

Keywords: remote sensing, phenology, paddy rice, time series MODIS EVI, growth monitoring, Savitzky-Golay filter, wavelet transform

DOI: 10.3965/j.ijabe.20140706.005

Citation: Li S H, Xiao J T, Ni P, Zhang J, Wang H S, Wang J X. Monitoring paddy rice phenology using time series MODIS data over Jiangxi Province, China. Int J Agric & Biol Eng, 2014; 7(6): 28－36.

1 Introduction

Rice is an important crop, as it occupies more than 11% of the world's cropland area and provides food for approximately 50% of the world's human population[1]. China is one of the major rice cultivation countries, which producing approximately one-third of the global rice crop[2]. The double rice cropping system (two rice crops in a year) in China is about 66% of the total paddy rice area[3], producing 61.3% of the total rice yield[4]. Estimation and monitoring of double-paddy rice phenology could provide important information for rice growth monitoring and yield prediction. Further, monitoring crop phenology across large areas is essential for the estimation of net primary production and crop yield[5]. The timing of crop planting and harvesting is important, as it also influences the spatial and inter-annual variability of terrestrial carbon cycles[6].

The phenological stage of crop can be measured using

Received date: 2014-09-09 **Accepted date:** 2014-12-02

Biographies: Xiao Jiangtao, Master, majoring in agricultural remote sensing. Email: jiangtao_xiao@163.com. **Ni Ping**, majoring in agricultural remote sensing. Email: 455836324@qq.com. **Zhang Jing**, Master, majoring in global change remote sensing. Email: zhangjing@nrscc.gov.cn. **Wang Hongshu**, majoring in vegetation remote sensing. Email: 524321325@qq.com. **Wang Jingxian,** majoring in vegetation remote sensing. Email: 951750248@qq.com.

* **Corresponding author: Li Shihua,** PhD, Associate Professor, majoring in remote sensing and its applications in agriculture and global change. Mailing address: No.2006, Xiyuan Ave, West Hi-Tech Zone, School of Resources and Environment, University of Electronic Science and Technology of China, Chengdu, 611731, China. Email: lishihua@uestc.edu.cn, Tel: +86-13551265998, Fax: +86-28-6183-1571.

field survey, simulated by bioclimatic models or detected with remotely sensed data[7] or carbon flux data[8-10]. Ground observation provides phenological data with high temporal resolution. Haw et al.[11] used colour vision to detect the rice maturity. Pei et al.[12] integrated sensor system for monitoring rice growth conditions based on unmanned ground vehicle system. However, Ground observation is difficult to extrapolate the data to large areas[13,14]. Bioclimatic models depend on the accuracy of the vegetation maps and climate records used as forcing variables at larger scales[7]. Remotely sensed data provide an opportunity to detect the phenological stages of crops at regional to global scales[13].

Time-series analysis of remote sensing data provides important information for estimating crop phenological stages. The most common approach is the utilization of vegetation indices (VI) such as normalized difference vegetation index (NDVI)[15] and enhanced vegetation index (EVI)[16] to detect crop phenology. Moderate Resolution Imaging Spectroradiometer (MODIS) has a 250-m spatial resolution in red and near infrared bands and minimizes the mixed-pixel effect that limits the application of the coarser resolution of 1-km data sets from the National Oceanic and Atmospheric Administration's Advanced Very High Resolution Radiometer (NOAA/AVHRR) and SPOT-VEGETATION[17-19]. MODIS time-series VI products are now used for building a MODIS global vegetation phenology product that provides detects of the timing of major seasonal vegetation events at global scales[20]. Sakamoto et al.[21] applied multi-temporal seasonal MODIS EVI data to detect the spatial distribution of heading date and rice-cropping system in the Mekong Delta relative to seasonal changes in water resources in 2002 and 2003. Motohka et al.[22] found that the most robust dataset for monitoring rice paddy phenology during monsoon in Asia is the daily EVI derived from a combination of Terra/MODIS and Aqua/MODIS. Boschetti et al.[23] used five years (2001–2005) data of MODIS NDVI 16-day composites to automatically retrieve key phenological parameters such as the start of season (emergence), peak (heading), and end of season (maturity). Wang et al.[24] identified the rice heading date and analyzed the spatial characteristics at the regional scale by using multi-temporal MODIS NDVI data. Xiao et al.[25] evaluated the MODIS phenological product during 2001 to 2009 in combination with ground-based phenological data for wheat/maize rotation systems in the North China Plain.

Time-series VI data derived from satellite data typically contain noise induced by cloud contamination, atmospheric variability, and bidirectional reflectance. Noise reduction or model fitting for observed data is necessary before determination of phenology stages. An effective method for data preprocessing is the utilization of a smoothing algorithm for noise reduction[5]. A number of methods for reducing noise and constructing high-quality VI time-series data have been developed and evaluated in the last decades. Existing studies suggest that the Savitzky–Golay filter and wavelet analysis are two robust algorithms that reduce noise in time series such as VI time series. The Savitzky–Golay filter reduces noise in NDVI time-series data, which is primarily caused by cloud contamination and atmospheric variability[26]. The wavelet transform also can be utilized to remove noise. The advantage of the wavelet transform is the feasibility of identifying the timing of events, e.g. localized objective signals, with the presence of noise[5]. Chen et al.[27] conducted rice cropland mapping using time-series MODIS data by wavelet filtering, and the study showed that good results can be achieved using wavelet transformation in cleaning rice signatures. Yang et al.[28] smoothed the hyperspectral imagery noise using several smoothed method which include wavelet, S-G method and other methods.

EVI has a greater dynamic range than NDVI, and therefore is more suitable for capturing dynamic crop phenology without saturation[16,29]. The main objectives of this study were to detect the paddy rice phenological stages (i.e. transplanting, tillering, heading, and harvesting) using smoothed MODIS EVI time-series and ground observation data. To reduce the noise and reconstruct the smoothed time-series profile, MODIS EVI time-series data were smoothed using the Savitzky–Golay filter and wavelet transform. The accuracy of estimation was assessed with ground observation data collected between 2006 and 2008 for 10 agricultural meteorological stations in Jiangxi Province, China.

2 Methods

2.1 Study area

Jiangxi Province is located in southern China from 24°29′-30°04′N and 113°34′-118°28′E. It is 166 900 km^2 and comprised of approximately 36% mountainous areas, 42% hills, and 22% mounds, plains, and water bodies. Poyang Lake is the largest basin in Jiangxi Province. This region has a typical humid subtropical climate, with sufficient sunshine, plentiful rainfall and a long frost-free period. In 2009, the average temperature of the province was 18.9°C, with 1 438.1 mm annual precipitation and 1 686.3 hours of sunshine[30].

Currently, there are nearly 400 agricultural meteorological stations operated by the Chinese Meteorological Agency (CMA) in China. At the agricultural meteorological stations, crops are observed at regular intervals. The resulting crop growth records provide detailed information about crop types and phenology. In this study, we used paddy rice phenology data collected at 10 agricultural meteorological stations in Jiangxi Province as ground validation data. Double-paddy rice was grown at all 10 stations, and each station monitored paddy rice area that was greater than 1 km^2 (Figure 1).

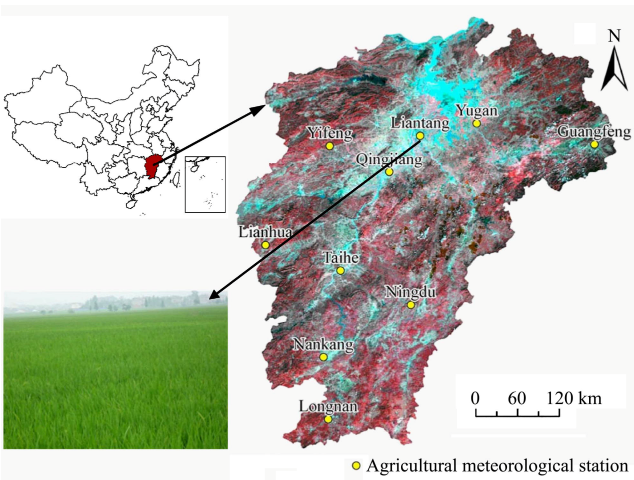

Figure 1 Study area and agricultural meteorological stations

2.2 Data Preprocessing

MOD09A1 8-day composite products with 500-m spatial resolution were used in this study. Four MODIS files (h27v05, h27v06, h28v05, and h28v06) from 2006 to 2008 cover Jiangxi Province were downloaded from the Earth Observing System Data Gateway. EVI values were calculated using surface reflectance values using the EVI equation:

$$\mathrm{EVI} = G \times \frac{\rho_{nir} - \rho_{red}}{\rho_{nir} + (C_1 \times \rho_{red} - C_2 \times \rho_{blue}) + L} \tag{1}$$

where, ρ_{blue}, ρ_{red}, and ρ_{NIR} are reflectance of MODIS blue, red, and near infrared bands, respectively; L (= 1) is the canopy background adjustment; C_1 (= 6) and C_2 (= 7.5) are aerosol resistance coefficients; and G (= 2.5) is a gain factor[16].

2.3 Reconstruction of VI time series

2.3.1 Savitzky–Golay filter

The Savitzky–Golay filter applies a simplified least-squares fit convolution method to smooth noisy time-series data[31]. The convolution is a weighted moving average filter with a polynomial of a certain degree. The weight coefficients (below referred to coefficients), when applied to a signal, perform a polynomial least-squares fit within the filter window. The polynomial is designed to preserve high order moments within the data and reduce the bias introduced by the filter. This filter can be applied to any consecutive data that has data points at fixed and uniform intervals along the chosen abscissa and curves formed by plotting the points that are continuous and more or less smooth. The general equation of the simplified least-square convolution for EVI time-series smoothing is described as Eq. (2)[26]:

$$Y_j^* = \frac{\sum_{i=-m}^{i=m} C_i Y_{j+i}}{N} \tag{2}$$

where, Y is the original EVI value; Y^* is the smoothed EVI value; C_i is the coefficient for the i^{th} EVI value of the filter (smoothing window); N is the number of convoluting integers, which is equal to the smoothing window size ($2m+1$); and j is the running index of the original ordinate data table.

Two parameters (m and d) must be defined in advance. The first parameter, m, is the half-width of the smoothing window. The second parameter, d, is an integer specifying the degree of the smoothing polynomial. In this study, d and m are 5 and 4, respectively.

2.3.2 Wavelet transform

Wavelet transform implements the decomposition of a signal at different spatial or time scales onto a set of basis functions. It has been widely applied in remote sensing data analysis[32,33]. The set of basis functions, $\{\psi_{a,b}(t)\}$, can be generated by translating and scaling the so-called mother wavelet, $\psi(t)$, according to the following equation[34,35]:

$$\psi_{a,b}(t)=\frac{1}{\sqrt{a}}\psi\left(\frac{t-b}{a}\right) \tag{3}$$

where, a is a scaling parameter and b is a shifting parameter. In discrete form, a and b are defined as:

$$(a,b)=(2^j,2^j k) \tag{4}$$

where, j and k are integral values[5].

Several mother wavelets have been proposed, e.g., Daubechies, derivative of Gaussian (DOG) and Coiflet[29,36]. The names of the Daubechies family of wavelets are written as dbN[37], where N is the order and db is the 'surname' of the wavelet[38]. In this study, db10 was applied to carry out the wavelet transform.

2.4 Estimating phenological stage

Generally, there are three types of methods to detect crop phenological stages: threshold-based methods, trend derivative methods, and inflection point methods[13,39]. The choice of a fixed threshold value is critical for defining phenology stages for environments[40]. We used features of time-series vegetation index (e.g., maximum value deviation) to extract key phenological dates.

As the heading time is the peak of the growth period, paddy rice also has maximum VI values and cover fractions in remote sensing images at heading time. Consequently, heading time can be detected as the maximum EVI value in the growing season of paddy rice. Because there are two peaks for double season rice, the heading time of early and late rice are indicated by the two time-series data peaks, EVI_{max1} and EVI_{max2}.

According to the seasonal trends and the peak values of EVI time-series data, EVI data can be divided into two stages: ascending and descending stages. EVI increases during the growth stage before heading. Because paddy rice is transplanted to the irrigation field and the plants are small during the transplanting period, remote sensing images reflect mainly water and soil. Therefore, the minimum values of EVI time-series profiles are at the start of the growth season. Paddy rice is in its most reproductive stage after heading, and EVI values decrease again to the minimum value at the time of the harvest. These changes permit the identification of transplantation times from EVI time series as follows: the date with minimum EVI before the peak value of first-season rice is the transplanting time for early rice and the time with minimum EVI between the two peaks of double-season rice is the transplanting time for late rice and the harvest time of early rice. The period with minimum EVI after the second heading is the harvest period for second-season paddy rice. It should be noted that the VI of paddy rice fields continues to decrease after harvest of second-season paddy rice, but before transplantation of first-season paddy rice. This results in different minimum EVI values for first-season transplanting and second-season harvest. In the present study, the rice growing season was defined as the period between pre-transplanting of first-season rice (16 days before transplanting) and post-harvest of second-season rice (16 days after harvest), e.g. day 90–320 of the year.

Tillering and harvesting can be identified with a flexible dynamic threshold method. Tillering begins approximately 10 days after transplanting and EVI rapidly increases. This means that tillering can be detected by defining the corresponding EVI threshold. By comparing thresholds of 5%, 10%, and 20%, we found that an increase of 10% of the difference between the maximum value and the minimum value during the EVI ascending curve is an appropriate threshold. We defined the start of tillering as the time when EVI increases above the threshold. Similarly, the start of harvesting was defined as the time when EVI decreased to below 10% of the difference between the maximum and minimum values. Tillering EVI (t_1) and maturation EVI (t_2) of early rice can be expressed as below:

$$\mathrm{EVI}(t_1)\geq \mathrm{EVI}_{\min 1}+10\%\times(\mathrm{EVI}_{\max 1}-\mathrm{EVI}_{\min 1}) \tag{5}$$

$$\mathrm{EVI}(t_2)\geq \mathrm{EVI}_{\min 2}+10\%\times(\mathrm{EVI}_{\max 1}-\mathrm{EVI}_{\min 2}) \tag{6}$$

The EVI_{min1} and EVI_{max1} are the minimum and maximum data of early rice, and the EVI_{min2} and EVI_{max2} are the minimum and maximum data of late rice (as showed in Figure 2).

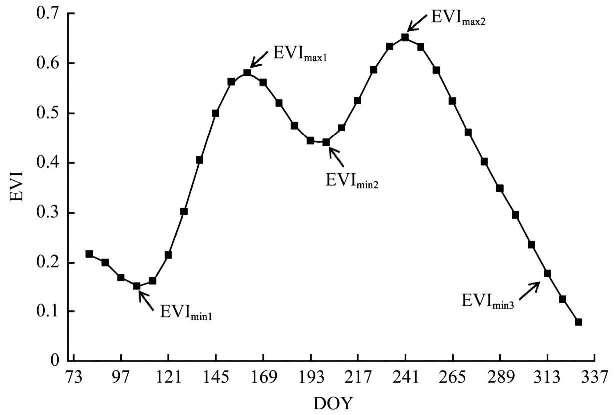

Note: DOY means day of year. The same below.

Figure 2 The EVI profile of double-cropping rice

3 Results and discussion

3.1 Comparison of results of Savitzky–Golay filter and wavelet transform

We compared the smoothed EVI time-series data obtained for Liantang Station and Qingjiang Station by using the Savitzky–Golay filter and wavelet transform (Figure 3). The phenology stages could be clearly identified from the general pattern of EVI time series. Most of the noise was successfully eliminated from the EVI time series. EVI values obtained by the Savitzky–Golay filter are greater than those obtained by the wavelet transform (Figure 3a and 3b), it is because the envelope data were used to fit the time series EVI. The Savitzky–Golay filter tends to retain the peak point data of EVI profile, e.g., the data values of the DOY 33 were retained using Savitzky–Golay filter (Figure 3b), whereas the wavelet filter smoothed EVI values were removed. Compared with the Savitzky–Golay filter smoothed data, EVI curves smoothed by wavelet filter keep the original shape of EVI data as well as minimized the difference between the original and smoothed EVI data, the wavelet filter also removed high frequency components on the same day.

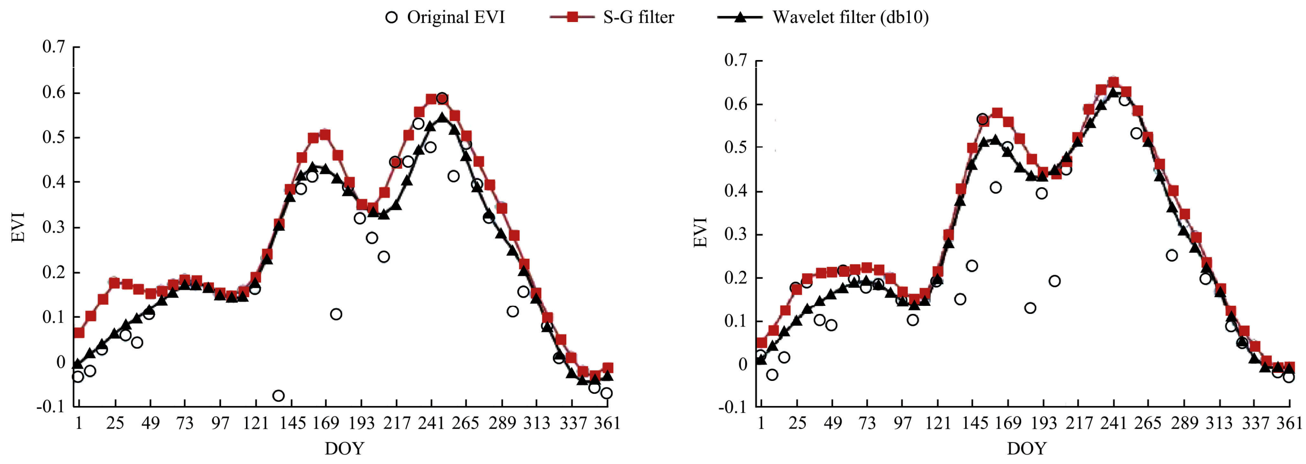

a. Liantang station

b. Qingjiang station

Figure 3 EVI time series generated using Savitzky–Golay and wavelet filter

3.2 Estimation of Phenology stages

The EVI time-series profile of Qingjiang Station in 2006 was selected for estimating key phenological dates for paddy rice. The Savitzky–Golay filtering algorithm was applied to process EVI time-series data. We can conclude from the Figure 4 that the first-season rice was transplanted between late April and early May, which matches the transplanting date derived from remote sensing data. After the second transplanting, paddy rice experienced the entire growth period until harvest in early November. The EVI time series reflected the changes in the morphological and physiological condition of the rice during this period. Thus, the dates of transplanting, tillering, heading, and maturation could be extracted from the remote sensing data using the phenology monitoring algorithms.

Key phenological dates of rice growth period only last a short time. The phenology dates identified using remote sensing data match well to every key stage of rice growth, and remotely sensed data can be adopted for monitoring rice-growing conditions.

With the comparison between remote sensing data and ground observations of early and late rice phenological stages, we can found the data can be similar or identical (Figure 5). The results indicate that the estimation of double-season rice phenological stages is feasible using time-series MODIS EVI data.

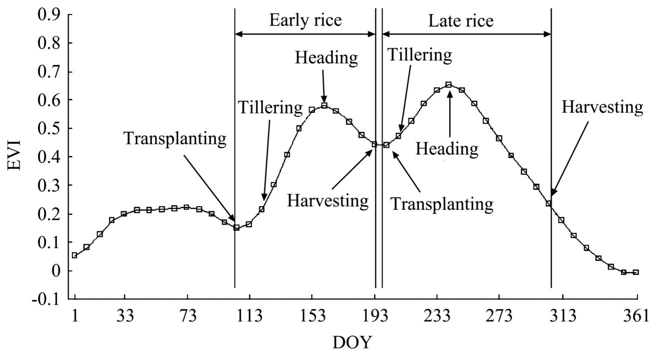

Figure 4 Phenological stages estimation of double paddy rice at Qingjiang station

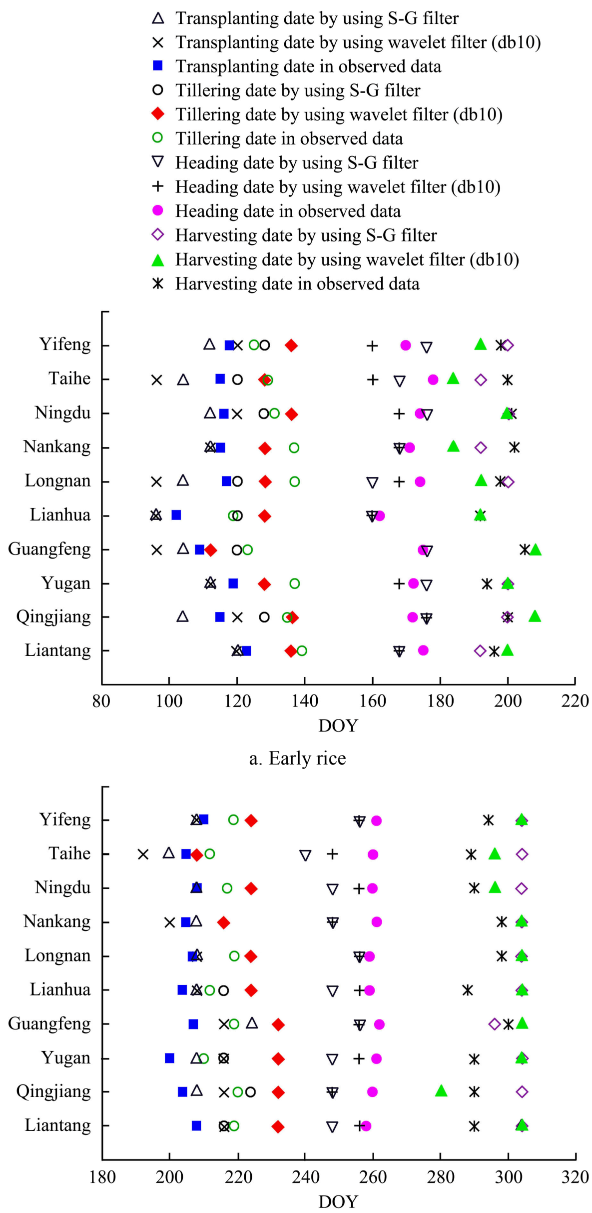

a. Early rice

b. Late rice.

Figure 5 Comparison between statistical data and the dates of phenological stages detected by methods using the Savitzky–Golay and wavelet filters

3.3 Accuracy assessment and analysis

The differences between the detected early and late paddy rice phenological dates with ground observation data for 10 agricultural meteorological stations from 2006 to 2008 were assessed (Figure 6). Twenty-two detected dates had errors of ±16 days (10% of dates) for early rice. For late rice, 18 sample dates (8% of dates) had errors that exceeded ±16 days.

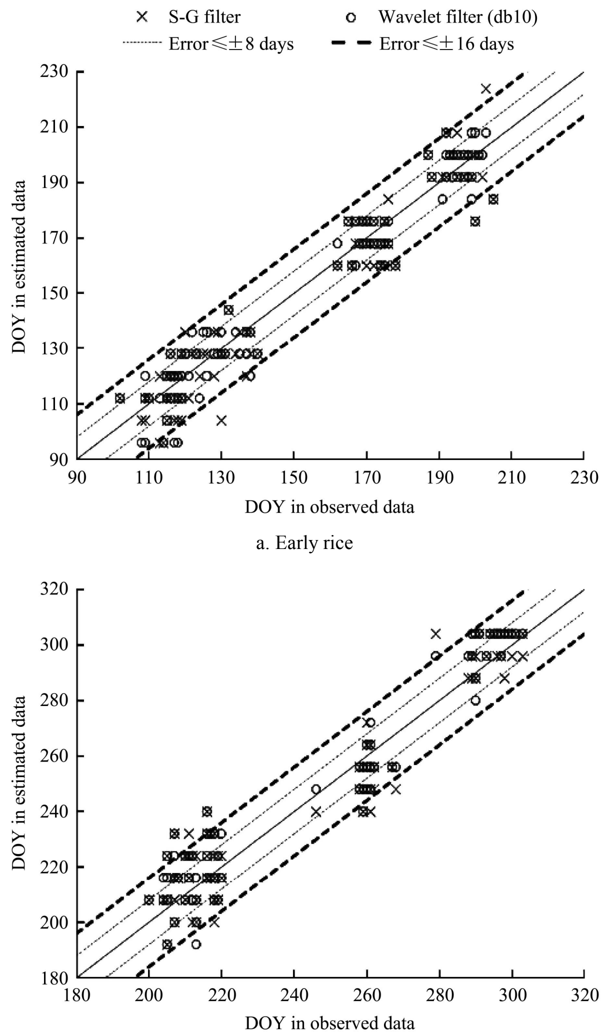

a. Early rice

b. Late rice

Figure 6 Comparison of phenological dates between ground observation data and MODIS-derived estimation in growing period

Table 1 shows the root mean square error (RMSE) of the detected phenological dates and ground observations. The error of detected early paddy rice phenological date with the Savitzky–Golay filter is larger than that achieved using the wavelet transform. However, the RMSE of late paddy rice phenology dates detected using the Savitzky–Golay filter is smaller than that obtained using the wavelet transform. The detected dates for each stage were generally within ±10 days of the ground observation data. The largest RMSE was obtained in the early rice transplanting period while the Savitzky–Golay filter was applied, and the smallest RMSE was obtained during the late rice transplanting period. For the same method, the RMSE of EVI value for early rice is lower than late rice results, it is because the late growth stage is in the summer and autumn seasons (July-October), it is most likely to occur during heavy rain, resulting in large errors of remote sensing monitoring results. The 8-day composite MODIS EVI data and the ground per day observation data have temporal resolutions, and the accuracy assessment using the "truth" acquired by ground observation should be improved in future studies.

Table 1 RMSE of detected phelonogy date and ground observation data

Days

	Reconstruction method	Transplanting	Tillering	Heading	Harvesting
Early rice	Savitzky–Golay filter	10	9	8	9
	wavelet transform	9	8	8	9
Late rice	Savitzky–Golay filter	8	12	11	8
	wavelet transform	9	13	10	9

The errors of remote sensing based phenological data may be induced by: (I) The remote sensing data are 8-day compositing MODIS data, and the ground phenological data were acquired with daily observations. That means the remote sensing based phenological data do not match the ground observations on temporal scale, and thereby reducing the accuracy of remote sensing phenology; (II) the spatial resolution of MODIS data used in this study is 500 m, and ground observations are acquired at the individual rice plants or small-scale fields. The spatial scales of remote sensing data and ground observations did not match very well. In summary, the temporal and spatial scale difference between the remote sensing data and ground observation data may introduce errors in the paddy rice monitoring.

4 Conclusions

Double-cropping rice occupies about two-thirds of the total paddy field area in China. Estimating the phenology of double-cropping rice is necessary for monitoring and managing rice growth. In this study, the phenological stages (i.e., transplanting, tillering, heading, and harvesting) of double-cropping rice in Jiangxi Province were detected using time-series MODIS EVI data. Three strategies were employed to analyze the EVI time-series profiles: (I) The EVI time-series data were reconstructed using the Savitzky–Golay filter and wavelet transform to monitor the phenology of paddy rice; (II) The feasibility and model for deriving key phenological stages for double-cropping rice such as transplanting, tillering, heading, and harvesting, by using MODIS EVI temporal profiles were investigated; and (III) The phenological-stage models were validated using ground observations from 10 agricultural meteorological stations, and their accuracies were analyzed.

The results suggest that both the Savitzky–Golay filter and wavelet transform are promising methods for reconstructing high-quality EVI time-series profiles. The key phenological dates detected from MODIS EVI time-series data have good agreement with ground observations acquired from the agricultural meteorological stations. The dates for each growing stage were generally detected within ±10 days of the ground observations. The difference of temporal and spatial scale between the MODIS data and ground observation data may be the main error sources of remote sensing based paddy rice monitoring. Thus, the phenological stages of double-cropping rice can be monitored well by using the reconstructed MODIS EVI time-series data. The key phenological date and the associated parameters could be used in crop management and yield estimation in precision agriculture.

Acknowledgments

We acknowlede that this work was supported by China's Special Funds for Major State Basic Research Project (2013CB733405), the Fundamental Research Funds for the Central Universities (ZYGX2012J153 and ZYGX2012Z005), the Open Fund of the State Key Laboratory of Remote Sensing Science (OFSLRSS201408) and the National Natural Science Foundation of China (40801130).

[References]

[1] Chen C F, Son N T, Chang L Y. Monitoring of rice cropping intensity in the upper Mekong Delta, Vietnam using time-series MODIS data. Adv. Space Res. 2012; 49(2): 292–301.

[2] Coats B. Global rice production. Rice origin, history, technology and production. Hoboken, NJ, USA: John Wiley and Sons, 2003; pp. 247–470.

[3] Bi L, Zhang B, Liu G, Li Z, Liu Y, Ye C, et al. Long-term effects of organic amendments on the rice yields for double rice cropping systems in subtropical China. Agric. Ecosyst. Environ., 2009; 129(4): 534–541.

[4] Liu L, Wang E, Zhu Y, Tang L, Cao W. Effects of warming and autonomous breeding on the phenological development and grain yield of double-rice systems in China. Agric. Ecosyst. Environ., 2013; 165: 28–38.

[5] Sakamoto T, Yokozawa M, Toritani H, Shibayama M, Ishitsuka N, Ohno H. A crop phenology detection method using time-series MODIS data. Remote Sens. Environ., 2005; 96(3): 366–374.

[6] Kang S, Running S W, Lim J H, Zhao M, Park C R, Loehman R. A regional phenology model for detecting onset of greenness in temperate mixed forests, Korea: an application of MODIS leaf area index. Remote Sens. Environ., 2003; 86(2): 232–242.

[7] Wu W, Yang P, Tang H, Zhou Q, Chen Z, Ryosuke S. Characterizing spatial patterns of phenology in cropland of China based on remotely sensed data. Agr. Sci. China, 2010; 9(1): 101–112.

[8] Garrity S R, Bohrer G, Maurer K D, Mueller K L, Vogel C S, Curtis P S. A comparison of multiple phenology data sources for estimating seasonal transitions in deciduous forest carbon exchange. Agric. For. Meteorol., 2011; 151(12): 1741–1752.

[9] Melaas E K, Richardson A D, Friedl M A, Dragoni D, Gough C M, Herbst M, et al. Using FLUXNET data to improve models of springtime vegetation activity onset in forest ecosystems. Agric. For. Meteorol., 2013; 171: 46–56.

[10] Wu C, Gonsamo A, Gough C M, Chen J M, Xu S. Modeling growing season phenology in North American forests using seasonal mean vegetation indices from MODIS. Remote Sens. Environ., 2014; 147: 79–88.

[11] Haw C L, Ismail W I W, Kairunniza-Bejo S, Putih A, Shamshiri R. Colour vision to determine paddy maturity. Int. J. Agric. & Biol. Eng., 2014; 7(5): 55–63.

[12] Pei W, Lan Y B, Luo X W, Zhou Z Y, Wang Z, Wang Y. Integrated sensor system for monitoring rice growth conditions based on unmanned ground vehicle system. Int. J. Agric. & Biol. Eng., 2014; 7(2): 75–81.

[13] Dash J, Jeganathan C, Atkinson P M. The use of MERIS Terrestrial Chlorophyll Index to study spatio-temporal variation in vegetation phenology over India. Remote Sens. Environ., 2010; 114(7): 1388–1402.

[14] Li B, Li L, Qin Y, Liang L, Li J, Liu Y, et al. Impacts of climate variability on streamflow in the upper and middle reaches of the Taoer River based on the Budyko Hypothesis. Resources Science, 2011; 33(1): 70–76. (in Chinese with English abstract)

[15] Tucker C J. Red and photographic infrared linear combinations for monitoring vegetation. Remote Sens. Environ. 1979; 8(2): 127–150.

[16] Huete A, Didan K, Miura T, Rodriguez E P, Gao X, Ferreira L G. Overview of the radiometric and biophysical performance of the MODIS vegetation indices. Remote Sens. Environ. 2002; 83(1): 195–213.

[17] Sakamoto T, Wardlow B D, Gitelson A A, Verma S B, Suyker A E, Arkebauer T J. A two-step filtering approach for detecting maize and soybean phenology with time-series MODIS data. Remote Sens. Environ., 2010; 114(10): 2146–2159.

[18] Zhang X, Friedl M A, Schaaf C B, Strahler A H, Hodges J C F, Gao F, et al. Monitoring vegetation phenology using MODIS. Remote Sens. Environ., 2003; 84(3): 471–475.

[19] Zhang X, Friedl M A, Schaaf C B. Global vegetation phenology from moderate resolution imaging spectroradiometer (MODIS): Evaluation of global patterns and comparison with in situ measurements. J. Geophys. Res., 2006; 111(G4): G04017.

[20] Hmimina G, Dufrêne E, Pontailler J Y, Delpierre N, Aubinet M, Caquet B, et al. Evaluation of the potential of MODIS satellite data to predict vegetation phenology in different biomes: An investigation using ground-based NDVI measurements. Remote Sens. Environ., 2013; 132: 145–158.

[21] Sakamoto T, Van Nguyen N, Ohno H, Ishitsuka N, Yokozawa M. Spatio–temporal distribution of rice phenology and cropping systems in the Mekong Delta with special reference to the seasonal water flow of the Mekong and Bassac rivers. Remote Sens. Environ., 2006; 100(1): 1–16.

[22] Motohka T, Nasahara K N, Miyata A, Mano M, Tsuchida S. Evaluation of optical satellite remote sensing for rice paddy phenology in monsoon Asia using a continuous in situ dataset. Int. J. Remote Sens., 2009; 30(17): 4343–4357.

[23] Boschetti M, Stroppiana D, Brivio P A, Bocchi S. Multi-year monitoring of rice crop phenology through time series analysis of MODIS images. Int. J. Remote Sens., 2009; 30(18): 4643–4662.

[24] Wang H, Chen J, Wu Z, Lin H. Rice heading date retrieval based on multi-temporal MODIS data and polynomial fitting. Int. J. Remote Sens. 2012; 33(6): 1905–1916.

[25] Xiao W, Sun Z, Wang Q, Yang Y. Evaluating MODIS phenology product for rotating croplands through ground observations. J. Appl. Remote Sens. 2013; 7(1): 073562–073562.

[26] Chen J, Jo¨nsson P, Tamura M, Gu Z, Matsushita B, Eklundh L. A simple method for reconstructing a high-quality NDVI time-series data set based on the Savitzky–Golay filter. Remote Sens. Environ., 2004; 91(3): 332–344.

[27] Chen C F, Son N T, Chen C R, Chang L Y. Wavelet filtering of time-series moderate resolution imaging spectroradiometer data for rice crop mapping using support vector machines and maximum likelihood classifier. J. Appl. Remote Sens., 2011; 5(1): 053525–053525-15.

[28] Yang H, Zhang D Y, Huang L S, Zhao J L. Wavelet-based threshold denoising for imaging hyperspectral data. Int. J. Agric. & Biol. Eng., 2014; 7(3): 36–42.

[29] Galford G L, Mustard J F, Melillo J, Gendrin A, Cerri C C, Cerri C E P. Wavelet analysis of MODIS time series to detect expansion and intensification of row-crop agriculture in Brazil. Remote Sens. Environ., 2008; 112(2): 576–587.

[30] About Jiangxi. http://english.jiangxi.gov.cn/AboutJiangxi/200808/t20080824_83092.htm.

[31] Savitzky A, Golay M J E. Smoothing and differentiation of data by simplified least squares procedures. Anal. Chem., 1964; 36(8): 1627–1639.

[32] Blackburn G A, Ferwerda J G. Retrieval of chlorophyll concentration from leaf reflectance spectra using wavelet analysis. Remote Sens. Environ. 2008; 112(4): 1614–1632.

[33] Wiman H, Qin Y. Fast Compression and Access of LiDAR Point Clouds Using Wavelets. In 2009 Joint Urban Remote Sensing Event, pp.718–723, Shanghai, China.

[34] Daubechies I. Ten lectures on wavelets. CBMS-NSF Regional Conference Series in Applied Mathematics 61, 1992; pp.377, PA: Soc. Ind. Appl. Math, Philadelphia.

[35] Martinez B, Gilabert M A. Vegetation dynamics from NDVI time series analysis using the wavelet transform. Remote Sens. Environ. 2009; 113(9): 1823–1842.

[36] Torrence C, Compo G P. A practical guide to wavelet analysis. B. Am. Meteorol. Soc. 1998; 79(1): 61–78.

[37] Misiti M, Misiti Y, Oppenheim G, Poggi J M. Wavelet Toolbox User's Guide. The Math Works Ins., 1996.

[38] Pu R, Gong P. Wavelet transform applied to EO-1 hyperspectral data for forest LAI and crown closure mapping. Remote Sens. Environ., 2004; 91(2): 212–224.

[39] Reed B C, Brown J F, Vanderzee D, Loveland T R, Merchant J W, Ohlen D O. Measuring phenological variability from satellite imagery. J. Veg. Sci., 1994; 5(5): 703–714.

[40] Boschetti M, Stroppiana D, Brivio P A, Bocchi S. Multi-year monitoring of rice crop phenology through time series analysis of MODIS images. Int. J. Remote Sens., 2009; 30(18): 4643–4662.